

ChemComm

Accepted Manuscript



This is an *Accepted Manuscript*, which has been through the Royal Society of Chemistry peer review process and has been accepted for publication.

Accepted Manuscripts are published online shortly after acceptance, before technical editing, formatting and proof reading. Using this free service, authors can make their results available to the community, in citable form, before we publish the edited article. We will replace this *Accepted Manuscript* with the edited and formatted *Advance Article* as soon as it is available.

You can find more information about *Accepted Manuscripts* in the [Information for Authors](#).

Please note that technical editing may introduce minor changes to the text and/or graphics, which may alter content. The journal's standard [Terms & Conditions](#) and the [Ethical guidelines](#) still apply. In no event shall the Royal Society of Chemistry be held responsible for any errors or omissions in this *Accepted Manuscript* or any consequences arising from the use of any information it contains.

COMMUNICATION

Unexpected Optical Limiting Properties from MoS₂ Nanosheets Modified by Semiconductive Polymer

Cite this: DOI: 10.1039/x0xx00000x

Min Zhao^a, Meng-Jie Chang^a, Qiang Wang^{a*}, Zhen-Tong Zhu^a, Xin-Ping Zhai^a,
Mohammad Zirak^b, Alireza Z. Moshfegh^b, Ying-Lin Song^{c*} and Hao-Li Zhang^{a*}

Received 00th January 2012,

Accepted 00th January 2012

DOI: 10.1039/x0xx00000x

www.rsc.org/

Direct solvent exfoliation of bulk MoS₂ with the assistance of poly(3-hexylthiophene) (P3HT) produces novel two-dimensional organic/inorganic semiconductor heterojunction. The obtained P3HT-MoS₂ nanohybrid exhibits unexpected optical limiting properties in contrast to the saturated absorption behavior of both P3HT and MoS₂, showing potential in the future photoelectric applications.

Atomically thin transition metal dichalcogenides (TMDs) has received considerable attention in recent years, because of their unusual electrical and optical properties when charge transport is confined to a plane¹. As the most common example of semiconducting TMDs, layered MoS₂ has attracted significant interest and has been extensively explored for various applications such as transistors^{1a, 2}, photoswitches³, and electrochemical catalysis⁴.

Many different methods have been reported to prepare thin MoS₂ nanosheets, such as mechanical exfoliation^{2a}, ion intercalation technique⁵, liquid exfoliation^{1d, 6} and chemical vapor deposition growth⁷. Among these methods, solution-phase exfoliation has the advantages of low-cost, scalable and does not alter their intrinsic electronic properties. Coleman et al. firstly reported the solvent exfoliation MoS₂ using high-boiling solvents^{1d, 8}. Our group have developed a liquid exfoliation protocol to obtain stable suspensions of 2D TMDs by solvent mixtures⁶. Exfoliation of MoS₂ in water is also possible when using ionic surfactants⁹, phosphonic acid calix[8]arene¹⁰, thiol-terminated ligands¹¹ or water soluble polymers¹² as dispersion reagents.

Atomically thin layered MoS₂ stands out from other materials as it shows high carrier motilities while maintains an intrinsic band gap. This feature makes 2D MoS₂ more suitable for optoelectronic applications than pristine graphene. Unfortunately, most of the preparation methods do not preserve the semiconductive properties of MoS₂. For instance, though lithium intercalation technique is very efficient in producing layered MoS₂ nanosheets, it converts the semiconductor into metal. While most of the polymer and small molecule dispersion reagents are insulators, which form insulating coating to the MoS₂ that is not desirable for optoelectronic applications. Preparation of MoS₂ nanostructures modified by organic semiconductors is a fascinating idea, because such new type of nanoscale inorganic/organic heterojunction may exhibit novel

optical or electronic properties.

Herein, we demonstrate for the first time that with addition of poly(3-hexylthiophene) (P3HT), a semiconductive polymer, bulk MoS₂ can be exfoliated into very thin flakes under sonication, forming a novel organic/inorganic nanohybrid. Direct contact between the P3HT and the MoS₂ ensure efficient energy and electron transport between the two semiconductors. The P3HT-MoS₂ nanohybrid exhibits superior nonlinear optical (NLO) response that is distinctly different from either MoS₂ or P3HT, making it a new candidate for NLO and optoelectronic devices.

The preparation of P3HT-MoS₂ nanohybrid via the polymer-assisted exfoliation process is schematically shown in Figure 1a. Briefly, the commercial available MoS₂ powder was sonicated in chloroform in the presence of P3HT and then purified by centrifugation. For comparison, we have also characterized the bulk MoS₂ powder, unmodified MoS₂ nanosheets prepared by liquid exfoliation in the mixture of water and ethanol⁶ and pure P3HT.

It has been reported previously that chloroform is not able to exfoliate MoS₂ efficiently⁸. As shown in figure 1b, in the absence of dispersing reagent, the MoS₂ flakes were hardly dispersed in chloroform even after long time sonication. In contrast, the P3HT-MoS₂ nanohybrid consisting nanoscale MoS₂ flakes coated by P3HT can be easily dispersed in chloroform and exhibit deep brown color (Figure 1b). The dispersed P3HT-MoS₂ nanohybrid can be separated from the solvent and dissolved P3HT by centrifugation followed by drying in vacuum to give black powder. The dried nanohybrid powder can be redispersed into a wide range of organic solvents, including carbon tetrachloride, tetrahydrofuran, toluene, o-dichlorobenzene, as long as they are good solvents for P3HT (Figure S1, ESI[†]). In contrast to unmodified MoS₂, the nanohybrid can hardly be dispersed in some high polar organic solvents, including 1-methyl-2-pyrrolidinone (NMP), dimethyl sulfoxide (DMSO) and dimethylformamide (DMF) that are good solvents for MoS₂ but are poor solvents for P3HT. The above results shows that that the solubility of the nanohybrid is dominated by the polymer but not by the MoS₂, suggesting that there is a high surface coverage of P3HT on the MoS₂ and the interaction between the two components is strong. Meanwhile, the color of P3HT-MoS₂ is much darker than the bright orange color of P3HT and is nearly the same to the unmodified MoS₂ nanosheets, indicating that the MoS₂ dominating the optical property in the visible range (Figure S2, ESI[†]).

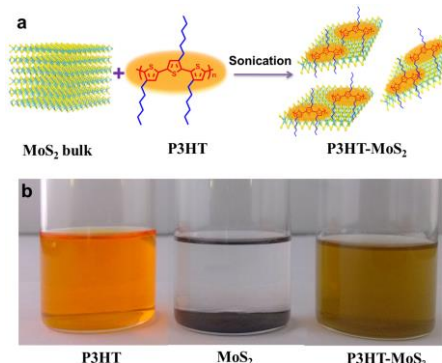


Figure 1. (a) Schematic illustration of P3HT-assisted exfoliation of MoS₂. (b) Photographs of dispersions for pure P3HT, MoS₂ and P3HT-MoS₂ nanohybrid.

The UV-visible absorption spectra of the unmodified MoS₂ nanosheets⁶, P3HT and P3HT-MoS₂ nanohybrid are illustrated in Figure 2a. The unmodified MoS₂ shows two discernible peaks at 614 nm and 673 nm, which are attributed to the direct excitonic transitions of MoS₂ with the energy split from valence band spin-orbital coupling¹³. These two “spin-orbital paired” peaks indicate the layered MoS₂ is dispersed in the solvent as 2H-phase. For the P3HT-MoS₂ dispersed in chloroform solution, the characteristic peaks of both 2H MoS₂ sheets and P3HT are observed, confirming that P3HT has been modified on the surface of the 2H structured MoS₂. The absorption spectra of P3HT-MoS₂ in other solutions also show that MoS₂ sheets are all in 2H phase (Figure S3, ESI[†]). In addition, X-ray photoelectron spectroscopy (XPS) data further confirmed the successful coating MoS₂ sheets by P3HT (Figure S6, ESI[†]).

Figure 2b compares the Raman spectra of bulk MoS₂, unmodified MoS₂ and the P3HT-MoS₂ nanohybrid. In each case, a number of well-defined peaks are observed in the region of 150-450 cm⁻¹. The Raman peaks of the bulk MoS₂ powder were 377 and 403 cm⁻¹. The pure MoS₂ nanosheets also show two distinct band features, including one at 382.6 cm⁻¹ arising from the in-plane E_{2g} vibration and the other at 407.5 cm⁻¹ arising from the out-of-plane A_{1g} vibration. The locations of these two peaks are in agreement with that reported for few-layer MoS₂^{8,14}. The Raman peaks of P3HT-MoS₂ nanohybrid are observed at 382.2 and 407.5 cm⁻¹ which are same to the unmodified MoS₂ nanosheets and are red-shifted in comparison with MoS₂ powder. The red-shift verifies the significant reduction of the flake thicknesses from the bulk MoS₂ to the dispersed samples^{8,13}. Figure S4a (ESI[†]) shows the XRD spectrum of the MoS₂ powder, in which the diffraction peaks located at 2θ = 14°, 33°, 40°, 50°, 59° corresponding to the planes of (002), (100), (103), (105) and (110), respectively, agreeing well with the hexagonal MoS₂ (JCPDS card No. 37-1492). While the survey of the P3HT-MoS₂ using X-ray diffraction (XRD) showed primary peak at 2θ = 14° (Figure S4b, ESI[†]), indicating the production of few layers did not change the structure of MoS₂.

Motivated by the exploration of electronic role of polymer P3HT and whether there exist electronic interaction between semiconductive polymer¹⁵ and MoS₂ nanosheets, we thereafter employ steady-state and time-resolved fluorescence spectroscopy to obtain an in-depth understanding. The steady-state fluorescence spectra were measured at the same excitation wavelength of 445 nm where the P3HT and P3HT-MoS₂ nanohybrid have similar absorbance. The fluorescence intensity of P3HT-MoS₂ nanohybrid is much lower than that of P3HT (Figure 2c) and the calculation of fluorescence quantum yield for P3HT-MoS₂ nanohybrid is 22 %,

which is about half of that of pure P3HT (37 %), suggesting the fluorescence quenching due to photo-induced electron and/or energy transfer between P3HT and MoS₂. We then studied the fluorescence decay of P3HT and P3HT-MoS₂ nanohybrid at the wavelength of 575 nm excited by 464 nm LED (Figure 2d). The major decay components were derived by single exponential data fitting. The reduced lifetime of P3HT-MoS₂ nanohybrid (0.55 ± 0.03 ns) compared with P3HT (0.68 ± 0.04 ns) further suggested the charge transfer process between the P3HT and MoS₂ nanosheets. Hence, both the steady-state and time-resolved fluorescence spectroscopy data indicate that MoS₂ nanosheets quenches fluorescence of conjugated polymers P3HT due to electronic coupling¹⁵.

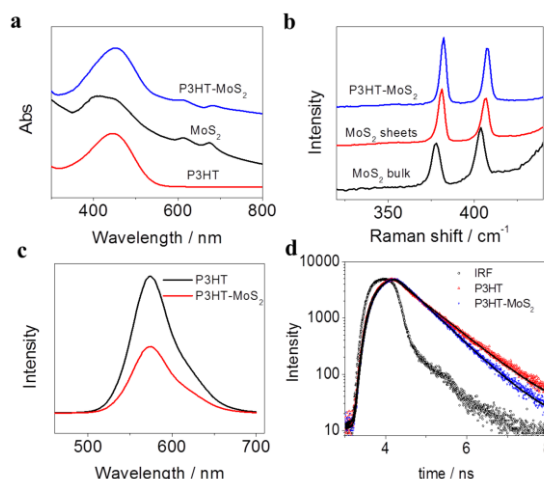


Figure 2. (a) UV/Vis absorption spectra of the unmodified MoS₂ nanosheets, pure P3HT and P3HT-MoS₂ nanohybrid. (b) Raman spectra of MoS₂ powder, pure MoS₂ nanosheets and P3HT-MoS₂ nanohybrid ($\lambda_{\text{ex}}=633$ nm). (c) Steady-state fluorescence spectra and (d) Time-resolved fluorescence spectra of P3HT and P3HT-MoS₂ nanohybrid in chloroform, where P3HT concentration was adjusted to be the same for comparison.

Figure 3a shows a representative transmission electron microscopy (TEM) image of typical flakes, which reveals that extremely thin MoS₂ flakes with the diameter of ~200 nm can be obtained via P3HT assisted exfoliation. As shown in Figure 3b and Figure S5d (ESI[†]), high-resolution TEM (HRTEM) and Scanning TEM (STEM) images of the as-synthesized P3HT-MoS₂ nanohybrid indicate well-defined atomic structure. The image intensity between neighboring atoms implies that the 2H structures of MoS₂ remain undistorted after ultrasonic preparation¹³, which is in good agreement with the above Raman results. Figure 3b shows the 0.27 nm interplane distance corresponding to the (100) planes, which are consistent with previously reported 2H phase¹⁶.

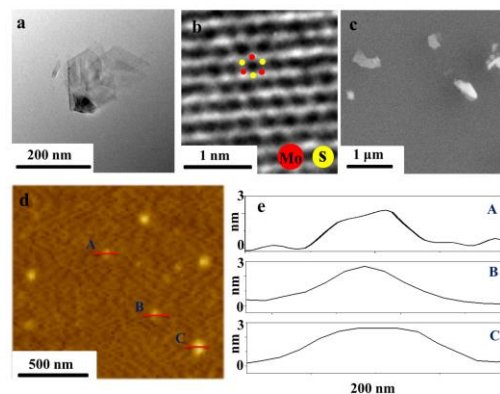


Figure 3. (a) Typical bright field TEM and (b) HRTEM images of P3HT-MoS₂ nanohybrid. (c) SEM images of P3HT-MoS₂ nanohybrid (d) AFM images and (e) Height profiles of P3HT-MoS₂ nanohybrid shown in (d).

To further study the size and thickness of the obtained P3HT-MoS₂ nanohybrid, Scanning Electron Microscope (SEM) Atomic Force Microscopy (AFM) measurement was performed (Figure 3c and 3d). As shown in Figure 3c, the obtained MoS₂ flakes have a distribution of lateral dimension between 50 nm to 400 nm, which is in accordance with that observed in AFM images shown in Figure 3d. It is noted that the AFM and SEM images somehow blur compared with that of pure MoS₂^{6,17}, which can be attributed to the presence of the soft polymer coated on the MoS₂ flake. The thickness of the MoS₂ sheets was around 2–4 nm measured from AFM image profile (Figure 3e). Considering that the thickness of a MoS₂ monolayer is about 0.65 nm¹⁸, the AFM data suggests that the nanohybrid contains less than 3 layers of MoS₂. It is noted that the layer number is likely to be overestimated, since the P3HT coated on the MoS₂ surface could contribute to the measured thickness.

We then studied how the photo-induced electronic coupling between P3HT and MoS₂ will affect the NLO properties of P3HT-MoS₂ nanohybrid. The NLO properties of MoS₂ dispersions have been reported only by a few groups, and show either saturable (SA) or reverse saturable absorption (RSA) behaviors depending on the preparation methods and the input laser fluence^{13, 16, 19}. Our group has previously revealed that NLO properties of modification-free TMD nanosheets are size-dependent¹⁷. Meanwhile, it is known from studies on graphene²⁰ that surface functionalization can be an effective approach to improve NLO properties of 2D materials. However, tuning the NLO properties of MoS₂ nanosheets by surface modification has not been investigated.

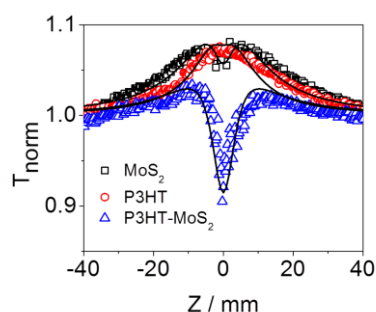


Figure 4. (a) Open aperture Z-scan data and theoretical fit curves using 4 ns pulses at 532 nm for all the samples with same linear transmittance of 0.81. T_{norm} is the measured transmittance normalized by the linear transmittance of the sample.

NLO characteristics of the different materials were measured using nanosecond Z-scan technique²¹. Laser pulses with pulse width of 4 ns full width at half maximum (FWHM) were generated from a frequency doubled and Q-switched Nd:YAG laser at the wavelength of 532 nm. The normalized transmittance of the sample was measured as a function of the incident laser fluence, which was varied by translating the sample through the focal plane along its propagation (Z) axis (more details in Figure S9, ESI†). For optical limiters, the measured curves would exhibit valleys at the focus and the deeper the valley, the stronger the optical limiting performance of the materials. Figure 4 displays the open aperture Z-scan data of unmodified MoS₂ in ethanol/water, P3HT and P3HT-MoS₂ nanohybrid dispersions with input laser pulse energy of 40 μJ . It could be found that at the same intensity, MoS₂ and P3HT mainly show SA properties, which is in accordance with the earlier works^{13, 19b, 22}. In contrast, the P3HT-MoS₂ nanohybrid displays a significant

reduction in the transmission, which means it show strong RSA behavior. Fitting the Z-scan data using equation 1 (ESI†) gives the nonlinear absorption coefficient of β value of $5.0 \times 10^{-11} \text{ m} / \text{W}$ for P3HT-MoS₂, which is three times larger than that of MoS₂ ($1.5 \times 10^{-11} \text{ m} / \text{W}$). All these results suggest that P3HT-MoS₂ hybrid has great potential as a type of excellent NLO material for optical limiting application. In addition, dependency of the nonlinear optical signal intensity against the incident light intensity was also investigated (Figure S7, ESI†).

The mechanism of NLO properties of nanomaterials is complicated by many factors, among them incident laser pulse and the intrinsic properties of the nanomaterials are the most important²³. Most of the light absorption in semiconductive nanomaterials is owing to the excitation of free carries²³. Consequently, when the free carries have been depleted, the absorption subsequently saturates with the appearance of the SA properties¹⁷. Meanwhile, for nanomaterials with high absorption cross section, the laser-induced heating could lead to solvent evaporation and micro bubble formation around the nano-materials. These micro bubbles then cause thermal induced nonlinear scattering with an appearance of RSA, which has been found in the case of carbon nanotubes²⁴, graphene and their hybrids²⁵. The lifetimes of the micro bubbles have been reported to be around several nanoseconds²⁶. In our study, the optical limiting properties of P3HT-MoS₂ nanohybrid are expected to stem from a combination of free carrier absorption and nonlinear scattering.

The strong optical limiting properties of P3HT-MoS₂ nanohybrid than its individual compartments is attributed to the highly efficient charge transfer between P3HT and MoS₂ when excited by the 532 nm laser. Figure 5 illustrates the proposed mechanism for the superior optical limiting performance of P3HT-MoS₂ nanohybrid, where the energy levels of P3HT are taken from literatures²⁷ and the energy level of MoS₂ is determined from electrochemical measurement (Figure S8, ESI†). When the 532 nm laser excites the P3HT and results in exciton generation, the photo-excited electron from the LUMO of the P3HT transfers to the conduction band of the MoS₂. Hence the free carrier absorption cross section of P3HT-MoS₂ nanohybrid will be enhanced to induce stronger optical limiting performance. Moreover, the energy is further transferred into solution from the large surface area of MoS₂. Then thermal energy generates a large quantity of bubbles which usually cause strong nonlinear scattering effect resulting into the drastic enhancement of optical limiting performance¹⁵.

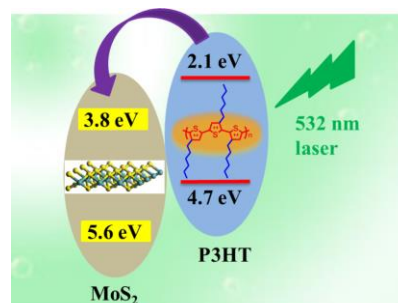


Figure 5. Schematic illustration of charge transfer between P3HT and MoS₂ sheets.

In summary, we have developed a facile method for exfoliation and dispersion of MoS₂ in organic solvents with the assistance of P3HT, which significantly improves the solubility and dispersion of the MoS₂ in organic solvents. Furthermore, unusually efficient optical limiting response of the nanohybrid

was discovered by Z-scan technique, which is in contrast to the saturated absorption behavior shown by the individual compartments. The distinct NLO properties of the P3HT-MoS₂ nanohybrid are attributed to the occurrence of photo-induced charge transfer between the P3HT and the MoS₂ nanosheets. The mechanism of the optical limiting properties is expected to arise from a combination of free carrier absorption and nonlinear scattering and this property makes the new 2D semiconductive hybrid a good candidate for use as optical limiter in photonic and optoelectronic devices.

This work is supported by National Basic Research Program of China (973 Program) No.2012CB933102, National Natural Science Foundation of China (NSFC. 21233001, 21190034, 21073079, J1103307), Specialized Research Fund for the Doctoral Program of Higher Education (SRFDP. 20110211130001), the Fundamental Research Funds for the Central Universities and 111 Project.

Notes and references

^a State Key Laboratory of Applied Organic Chemistry, Key Laboratory of Special Function Materials and Structure Design (MOE), College of Chemistry and Chemical Engineering, Lanzhou University, Lanzhou 730000, P. R. China

E-mail: haoli.zhang@lzu.edu.cn; qiangwang@lzu.edu.cn;

^b Department of Physics, Instit. for Nanosci. and Nanotechnol., Sharif University of Technology, P. O. Box 14588-89694. Tehran, Iran.

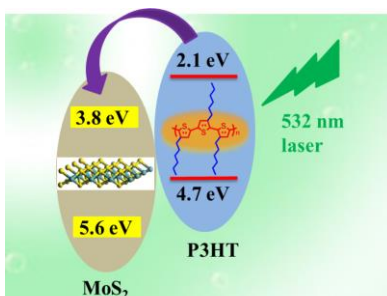
^c School of Physical Science and Technology, Soochow University, Suzhou 215006, P. R. China

E-mail: ylsong@hit.edu.cn

† Electronic Supplementary Information (ESI) available. See DOI: 10.1039/c000000x/

- (a) X. Huang, Z. Zeng and H. Zhang, *Chem Soc Rev*, 2013, **42**, 1934–1946; (b) M. Chhowalla, H. S. Shin, G. Eda, L.-J. Li, K. P. Loh and H. Zhang, *Nat. Chem.*, 2013, **5**, 263; (c) Q. H. Wang, K. Kalantar-Zadeh, A. Kis, J. N. Coleman and M. S. Strano, *Nat. Nanotechnol.*, 2012, **7**, 699; (d) V. Nicolosi, M. Chhowalla, M. G. Kanatzidis, M. S. Strano and J. N. Coleman, *Science*, 2013, **340**, 1420.
- (a) Z. Yin, H. Li, H. Li, L. Jiang, Y. Shi, Y. Sun, G. Lu, Q. Zhang, X. Chen and H. Zhang, *ACS Nano*, 2012, **6**, 74; (b) H. S. Lee, S.-W. Min, Y.-G. Chang, M. K. Park, T. Nam, H. Kim, J. H. Kim, S. Ryu and S. Im, *Nano Lett.*, 2012, **12**, 3695.
- K. Roy, M. Padmanabhan, S. Goswami, T. P. Sai, G. Ramalingam, S. Raghavan and A. Ghosh, *Nat. Nanotechnol.*, 2013, **8**, 826.
- D. Voiry, M. Salehi, R. Silva, T. Fujita, M. Chen, T. Asefa, V. B. Shenoy, G. Eda and M. Chhowalla, *Nano Lett.*, 2013, **13**, 6222.
- (a) D. Yang and R. F. Frindt, *J. Phys. Chem. Solids*, 1996, **57**, 1113; (b) Z. Zeng, Z. Yin, X. Huang, H. Li, Q. He, G. Lu, F. Boey and H. Zhang, *Angew. Chem. Int. Ed.*, 2011, **50**, 11093.
- K. G. Zhou, N. N. Mao, H. X. Wang, Y. Peng and H. L. Zhang, *Angew. Chem. Int. Ed.*, 2011, **50**, 10839.
- K.-K. Liu, W. Zhang, Y.-H. Lee, Y.-C. Lin, M.-T. Chang, C. Su, C.-S. Chang, H. Li, Y. Shi, H. Zhang, C.-S. Lai and L.-J. Li, *Nano Lett.*, 2012, **12**, 1538.
- J. N. Coleman, M. Lotya, A. O'Neill, S. D. Bergin, P. J. King, U. Khan, K. Young, A. Gaucher, S. De, R. J. Smith, I. V. Shvets, S. K. Arora, G. Stanton, H. Y. Kim, K. Lee, G. T. Kim, G. S. Duesberg, T. Hallam, J. J. Boland, J. J. Wang, J. F. Donegan, J. C. Grunlan, G. Moriarty, A. Shmeliov, R. J. Nicholls, J. M. Perkins, E. M. Grieveson, K. Theuvsissen, D. W. McComb, P. D. Nellist and V. Nicolosi, *Science*, 2011, **331**, 568.
- R. J. Smith, P. J. King, M. Lotya, C. Wirtz, U. Khan, S. De, A. O'Neill, G. S. Duesberg, J. C. Grunlan, G. Moriarty, J. Chen, J. Wang, A. I. Minett, V. Nicolosi and J. N. Coleman, *Adv. Mater.*, 2011, **23**, 3944.
- X. Chen, R. A. Boulos, P. K. Eggers and C. L. Raston, *Chem. Commun.*, 2012, **48**, 11407.
- S. S. Chou, M. De, J. Kim, S. Byun, C. Dykstra, J. Yu, J. Huang and V. P. Dravid, *J. Am. Chem. Soc.*, 2013, **135**, 4584.
- (a) J. Liu, Z. Zeng, X. Cao, G. Lu, L.-H. Wang, Q.-L. Fan, W. Huang and H. Zhang, *Small*, 2012, **8**, 3517; (b) T. Liu, C. Wang, X. Gu, H. Gong, L. Cheng, X. Shi, L. Feng, B. Sun and Z. Liu, *Adv. Mater.*, 2014, **26**, 3433.
- K. Wang, J. Wang, J. Fan, M. Lotya, A. O'Neill, D. Fox, Y. Feng, X. Zhang, B. Jiang, Q. Zhao, H. Zhang, J. N. Coleman, L. Zhang and W. J. Blau, *ACS Nano*, 2013, **7**, 9260.
- S. Tongay, J. Zhou, C. Ataca, K. Lo, T. S. Matthews, J. Li, J. C. Grossman and J. Wu, *Nano Lett.*, 2012, **12**, 5576.
- M. Shanmugam, T. Bansal, C. A. Durcan and B. Yu, *Appl. Phys. Lett.*, 2012, **100**, 153901.
- L. Tao, H. Long, B. Zhou, S. F. Yu, S. P. Lau, Y. Chai, K. H. Fung, Y. H. Tsang, J. Yao and D. Xu, *Nanoscale*, 2014, **6**, 9713.
- K. G. Zhou, M. Zhao, M. J. Chang, Q. Wang, X. Z. Wu, Y. Song and H. L. Zhang, *Small*, 2015, **11**, 694.
- B. Radisavljevic, A. Radenovic, J. Brivio, V. Giacometti and A. Kis, *Nat. Nanotechnol.*, 2011, **6**, 147.
- (a) S. Wang, H. Yu, H. Zhang, A. Wang, M. Zhao, Y. Chen, L. Mei and J. Wang, *Adv. Mater.*, 2014, **26**, 3538; (b) K. Wang, Y. Feng, C. Chang, J. Zhan, C. Wang, Q. Zhao, J. N. Coleman, L. Zhang, W. Blau and J. Wang, *Nanoscale*, 2014, **6**, 10530.
- (a) X. J. Xu, D. X. Ou, X. L. Luo, J. Chen, J. J. Lu, H. B. Zhan, Y. Q. Dong, J. G. Qin and Z. Li, *J. Mater. Chem.*, 2012, **22**, 22624; (b) W. Wei, T. He, X. Teng, S. Wu, L. Ma, H. Zhang, J. Ma, Y. Yang, H. Chen, Y. Han, H. Sun and L. Huang, *Small*, 2012, **8**, 2271; (c) Y. F. Xu, Z. B. Liu, X. L. Zhang, Y. Wang, J. G. Tian, Y. Huang, Y. F. Ma, X. Y. Zhang and Y. S. Chen, *Adv. Mater.*, 2009, **21**, 1275.
- M. Sheikbaha, A. A. Said, T. H. Wei, D. J. Hagan and E. W. Vanstryland, *IEEE Journal of Quantum Electronics*, 1990, **26**, 760.
- A. Martinez and Z. Sun, *Nat. Photonics*, 2013, **7**, 842.
- L. W. Tutt and T. F. Boggess, *Progress in Quantum Electronics*, 1993, **17**, 299.
- B. Anand, R. Podila, P. Ayala, L. Oliveira, R. Philip, S. S. Sai, A. A. Zakhidov and A. M. Rao, *Nanoscale*, 2013, **5**, 7271.
- (a) M. Feng, H. B. Zhan and Y. Chen, *Appl. Phys. Lett.*, 2010, **96**, 033107; (b) M. K. Kavitha, H. John, P. Gopinath and R. Philip, *J. Mater. Chem. C*, 2013, **1**, 3669.
- V. Kotaidis, C. Dahmen, G. von Plessen, F. Springer and A. Plech, *J. Chem. Phys.*, 2006, **124**, 184702.
- D. N. Congreve, J. Lee, N. J. Thompson, E. Hontz, S. R. Yost, P. D. Reusswig, M. E. Bahlke, S. Reineke, T. Van Voorhis and M. A. Baldo, *Science*, 2013, **340**, 334.

TOC: Unexpected Optical Limiting Properties from MoS₂ Nanosheets Modified by Semiconductive Polymer



We have developed a facile method for exfoliation of MoS₂ with the assistance of P3HT to synthesize P3HT-MoS₂ nanohybrid which show unexpected optical limiting properties compared with the individual compartments.